VOL 4, NO.2 (2024) 151-168
https://jagst.utm.my

JAGST
Journal of Advanced Geospatial Science & Technology

Multi-temporal Image Analysis for Land Cover Classification and Change Detection of Kuching Division, Sarawak

Hana Mohamed Jamil[1*], Nurul Suliana Ahmad Hazmi[1], Maizaitoldura Mohd Isa[1], Norimaniah Mazelan[1], Nur Amani Yusoff [1], Hazil Sardi Soliano[1], Ramzi Abdillah[2], Stephen Ling Jin Huat[2], Tony Octovius Ajol[2]

[1]Malaysian Space Agency (MYSA), No. 13, Jalan Tun Ismail, 50480 Kuala Lumpur, Malaysia
[2]Land and Survey Department, Sarawak (LSD), Level 6, Menara Pelita, Jalan Tun Abdul Rahman Yaakub, 93050 Petrajaya, Kuching, Sarawak, Malaysia

*Corresponding author: hana@mysa.gov.my

Abstract – Kuching and its surrounding area are vital in Sarawak's economic growth. Over the years, the transformation of its land cover (LC) has brought significant ecological, physical, and socioeconomic consequences. Updated and precise LC maps are essential for urban planning, sustainable development, and environmental forest degradation monitoring. This study mainly focuses on LC classification using the Support Vector Machine Classifier (SVM) algorithm. The change has been identified for five general classes, which are Urban Land, Barren Land, Forest Land, Agriculture Land, and Water Bodies, for 35 years using Landsat 5 TM image dated 26 June 1988 and Landsat 9 OLI image dated 16 April 2023 in ArcGIS 10.6.1 software. Change detection analysis indicated that from 1988 to 2023, the LC patterns changed significantly. The most substantial changes were urban land, which increased significantly from 6,200.71 ha in 1988 to 22,144.76 ha in 2023, which represents a net increase of 15,944.05 ha or 3.88 per cent change (%), followed by agriculture land, barren land, forest land, and water bodies categories. The results show good classification performance because the user's accuracy for every class is above 85%. LC change, which displays the spatial expansion of the urban land in Kuching, indicates the development of Sarawak is in line with the aspiration to be a developed state by 2030 (Post COVID-19 Development Strategy 2030).

Keywords *– Land cover, classification, change detection, multi-temporal*

Article History: Received 1 April 2024, Accepted 15 August 2024, Published 31 August 2024

How to cite: Mohamed Jamil, H., Ahmad Hazmi, N. S., Mohd Isa, M., Mazelan, N., Yusoff, N. A., Soliano, H. S., Abdillah, R., Stephen, L. J. H. and Tony, O. A. (2024). Multi-temporal Image Analysis for Land Cover Classification and Change Detection of Kuching Division, Sarawak. Journal of Advanced Geospatial Science and Technology. 4(2), 151-168.

1.0 Introduction

The changes in the land cover of an area are complex outcomes influenced by a combination of natural and socioeconomic factors over time and space (Dires Tewabe & Temesgen Fentahun, 2020). Land cover change monitoring involves detecting and analyzing changes in land cover over time. This process is important for understanding the land surface, managing natural resources, and assessing the impact of human activities on the environment (Roy and Roy, 2010). Land cover is also crucial for sustainable land resource planning and understanding changes in hydrological processes to meet the growing demand for basic needs and human welfare (Dires Tewabe & Temesgen Fentahun, 2020). Remote sensing satellites provide regular and consistent data acquisitions, enabling researchers to monitor changes over time. This temporal resolution facilitates the analysis of trends, patterns, and seasonal variations in land cover (Roy and Roy, 2010). Remote sensing sensors capture multispectral and hyperspectral data, allowing for the identification and classification of different land cover types. This data is used to create detailed land cover maps, providing valuable insights into the composition of urban planning. Conventional mapping methods, which involve manual records and field surveys where teams physically visit locations to collect data on land cover, topography, and existing maps, can be time-consuming and expensive, especially for large areas (Vivekananda, 2021). Remote sensing offers many advantages over traditional data acquisition methods by collecting data over large areas relatively quickly and providing valuable information more efficiently, timely, and cost-effectively (Vivekananda, 2021). Landsat data sets, with their medium-resolution capabilities, historical archives, and cost-free accessibility, have become a cornerstone for land cover change detection analyses worldwide. Their role in providing valuable information for monitoring Earth's surface changes over time is significant, contributing to the environment and supporting various land management and planning applications. Landsat data sets can be obtained free of charge from the United States Geological Survey (USGS) Earth Explorer online portal (http://earthexplorer.usgs.gov) (Vivekananda, 2021).

Kuching, the capital of Sarawak, Malaysia, was chosen as the study area due to rapid changes in land use/land cover activities. This study aims to produce land cover maps for 1998 and 2023, followed by a comprehensive analysis of changes over 35 years using remote sensing and Geographic Information Systems (GIS). Support Vector Machine (SVM) is often used to classify land cover, detect features, or analyze patterns in satellite imagery (Rokni, 2014). In addition, using the Support Vector Machine (SVM) algorithm for the land cover classification approach involves

several steps, such as data preparation, classifier training, land cover classification for both years and change detection analysis. The main contribution of this article is to analyze land cover in Kuching, Sarawak, Malaysia, using multiple temporal Landsat images. This localized study provides valuable insights into the impact of urban expansion, forest changes, and agricultural shifts on this division, which is crucial for local policymakers and urban planners. This study focuses on the whole division of Kuching, whereas the previous study from Kemarau, 2021, concentrates specifically on the city area of Kuching. Compared to the unsupervised technique applied by Kemarau, the SVM methodology produces better accuracy.

2.0 Study Area

Sarawak is one of the states of Malaysia situated on the island of Borneo. The total area of Sarawak is 12416972.17 ha. Sarawak consists of twelve divisions, one of which is Kuching, which is also its state capital. Kuching comprises three districts (Lundu, Kuching, and Bau) and two sub-districts (Padawan and Sematan). The total area of Kuching is 410878.83 ha. In 2020, the total population of Kuching recorded was 812,900 [Reference from Sarawak.gov.my website]. Kuching (Figure 1) has been selected as our study area primarily due to its rapid changes in land use activities.

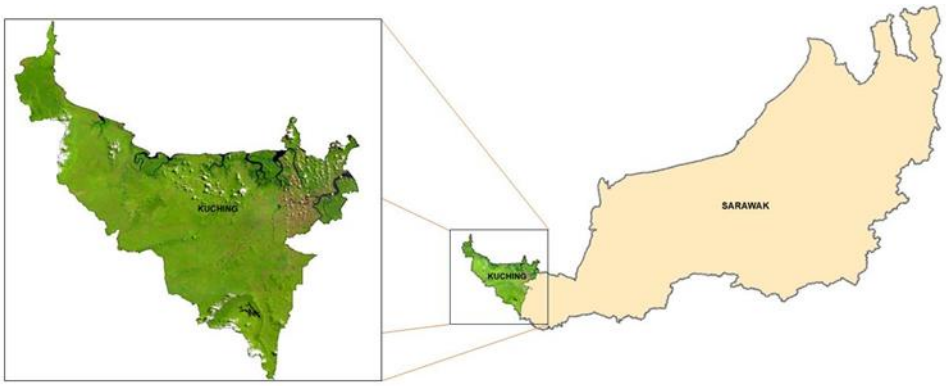

Figure 1. Study area.

3.0 Methodology

This study used remote sensing satellite imageries to interpret land cover change detection. Landsat 5 TM image dated 26 June 1988 and Landsat 9 OLI image dated 16 April 2023 were classified using the Supervised Classification method. The LC maps produced were then compared for change detection analysis. In this study, the methodology adopted was as follows: (1) Data

Acquisition, (2) Image Pre-processing, (3) Selection of Training Samples, (4) Image Classification, (5) Accuracy Assessment, and (6) Change Detection. The methodology flow chart is shown in Figure 2. All the processing involved, supervised classification, generating points for accuracy assessment purposes, and post-classification change detection comparison method were performed using ArcMap 10.8 software.

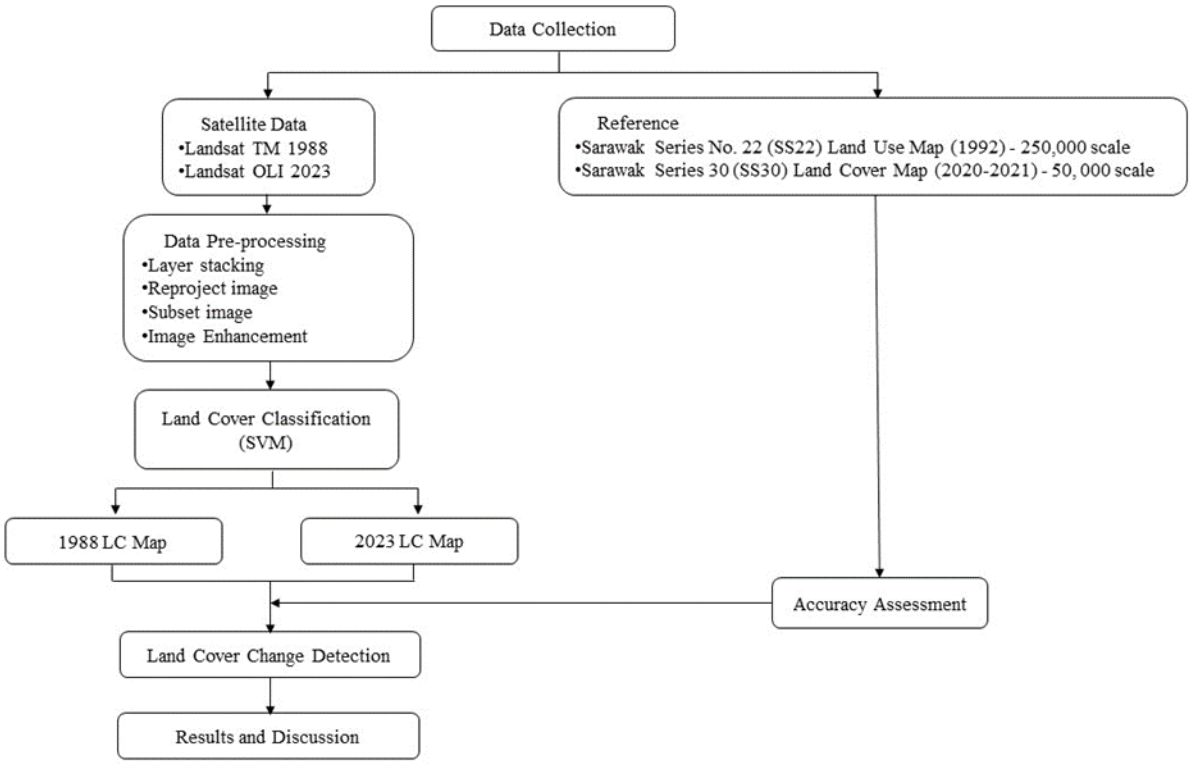

Figure 2. Methodology flow chart.

3.1 Data Acquisition

Landsat imageries with the Path/Row of 121/059 were used in this study area. Level 2 Landsat 5 Thematic Mapper (TM) image and Level 2 Landsat 8 and 9 image of Operational Land Imager (OLI) sensor were downloaded from the United States Geological Survey (USGS) Earth Explorer website (http://earthexplorer.usgs.gov). The images chosen were the best, with the least cloud cover. Information about the imageries used is shown in Table 1.

Table 1. Information on the imageries used.

Satellite	Date	Band Name	Wavelength Range (µm)	Resolution (m)
Landsat 5 TM	26 Jun 1988	Band 1 Blue	0.45 - 0.52	30
		Band 2 Green	0.52 - 0.60	30
		Band 3 Red	0.63 - 0.69	30
		Band 4 NIR	0.76 - 0.90	30
		Band 5 NIR	1.55 - 1.75	30
		Band 6 TIR	10.40 - 12.50	120
		Band 7 MIR	2.08 - 2.35	30
Landsat 9 OLI	16 April 2023	Band 1 Coastal Aerosol	0.43 - 0.45	30
		Band 2 Blue	0.45 - 0.51	30
		Band 3 Green	0.53 - 0.59	30
		Band 4 Red	0.64 - 0.67	30
		Band 5 NIR	0.85 - 0.88	30
		Band 6 SWIR 1	1.57 – 1.65	30
		Band 7 SWIR 2	2.11 – 2.29	30
		Band 8 Panchromatic	0.50 - 0.68	15
		Band 9 Cirrus	1.36 – 1.38	30
		Band 10 TIR	10.6 – 11.19	100
		Band 11 TIR	11.5 – 12.51	100

3.2 Image Pre-Processing

The imageries were stacked using the Band Composite function in ArcGIS. Then, they were reprojected to Borneo RSO (Rectified Skew Orthomorphic). Both scenes were subset according to the Kuching Division boundary obtained from the Land and Survey Department, Sarawak. The 410,878.83-hectares subset images of 1988 and 2023 are shown in Figures 3(a) and 3(b), respectively. These images were used for land cover classification and subsequent analysis.

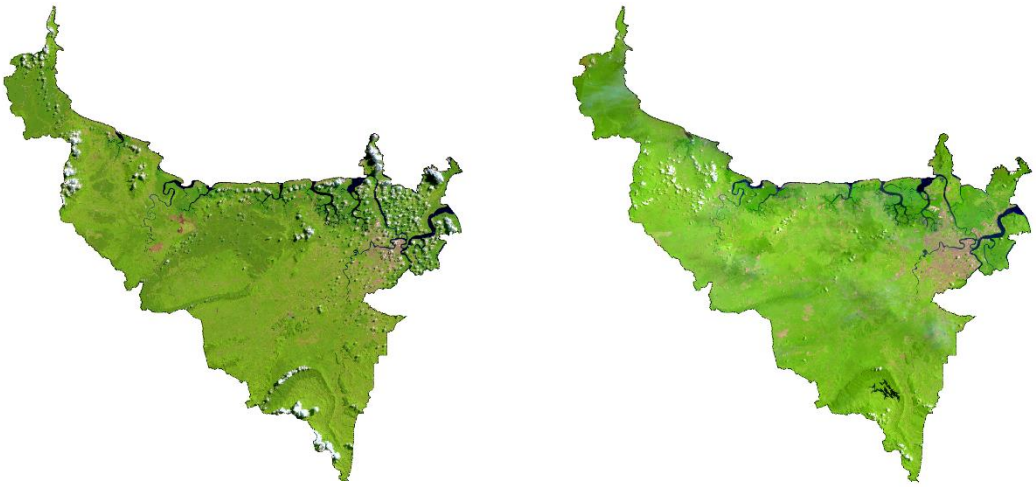

(a) (b)

Figure 3. (a) False Color Composite (FCC) 1988 Landsat 5 TM image of the study area. (b) FCC 2023 Landsat 9 OLI image of the study area.

3.3 Selection of Training Samples

In supervised classification, training samples are used to identify classes and calculate their signatures (ESRI, 2021). Training samples were created using the training sample drawing tools on the Image Classification toolbar. Band combinations 5, 4, and 3 were used for feature analysis. Data sets were trained according to the tone of the pixel colour.

3.4 Image Classification

The study area was broadly classified into five general classes: urban land, barren land, forest land, agricultural land, and water bodies, using a Support Vector Machine Classifier (SVM). A detailed description of the classes is provided in Table 2. Each class was derived according to texture, tone, and colour (Radhakrishnan et al., 2014). According to the study by Nurul et al. (2021) and Abbas et al. (2014)), the SVM classifier has higher accuracy than the MLC algorithm in land cover mapping.

Table 2. Area information for 1988 and 2023 classification categories.

Class	Year			
	1988		2023	
	Hectares (ha)	Percentage (%)	Hectares (ha)	Percentage (%)
Agriculture Land	201,225.76	48.97	186,642.53	45.43
Barren Land	15,240.31	3.71	9,951.95	2.42
Forest Land	178,369.48	43.41	181,446.65	44.16
Urban Land	6,200.71	1.51	22,144.76	5.39
Water Bodies	9,842.57	2.40	10,692.94	2.60
Total area	410,878.83			

The SVM is a non-parametric classifier. The success of the SVM depends on how well the process is trained. The easiest way to train the SVM is by using linearly separable classes. (Abbas *et al.,* 2014). According to Osuna *et al.* (1977), if the training data with **k** number of samples is represented as {Xi, Yi}, i =1,2,...,k where X € Rn is an n-dimensional space and y € {−1, +1} is a class label. These classes are considered linearly separable if a vector W exists perpendicular to the linear hyper-plane (which determines the direction of the discriminating plane), and **a** scalar **b** shows the offset of the discriminating hyper-plane from the origin. For the 2 classes, i.e. class 1 represented as −1 and class 2 represented as +1, 2 hyper-planes can be used to discriminate the data points in the respective classes. These are expressed as;

$$WXi + b \geq +1 \text{ for all } y = +1, \text{ i. e. a member of class 1} \quad (1)$$

$$WXi + b \leq -1 \text{ for all } y = -1, \text{ i. e. a member of class 2} \quad (2)$$

3.5 Accuracy Assessment

Classification accuracy assessment is an essential step after image classification. (Vivekananda *et al.,* 2020). According to Congalton and Green (1999), as a general rule of thumb, a minimum of 50 sample points per category is recommended, increasing to 75-100 sample points per category if you have large numbers of categories (> 12). For each 1988 and 2023 image set, the accuracy assessment tool of the supervised classifier randomly generated 260 and 253 reference points,

respectively, using the stratified random sampling method. The software immediately identified each point with a colour and pixel value (Mahadi *et al.,* 2023). The stratified random sampling creates points randomly distributed within each class, and each class has several points proportional to its relative area.

3.6 Change Detection

Remote sensing and GIS-based change detection approaches are widely used due to their cost-effectiveness and high temporal resolution (Vivekananda *et al.,* 2020). The post-classification comparison technique includes classifying imageries and comparing the relevant classes. This was conducted by converting the classified raster images into vector layers. To calculate the degree of change (C) for each class, the following equation was used:

$$Ci = Li - Bi \quad (3)$$

The change in class is divided by the covered area base year and multiplied by 100, the computation used to calculate the percentage of change (C%) (Vivekananda *et al.,* 2020). This process was conducted in each land cover class.

$$Pi = Li - Bi\ Bi \times 100 \quad (4)$$

The number of classes in the image is indicated by **I**. **Ci** indicates how much class **I** have changed. **Pi** is the percentage change in class **I** (Vivekananda *et al.,* 2020). **Li** is the earlier image (1988), while the most current image is **Bi** (2023).

4.0 Results and Discussion

The accuracy assessment results for the two data sets are shown in Tables 3 and 4. The area information for each class in both years was obtained from the attribute table. A post-classification comparison technique was performed, where the LC map 1988 was compared with the 2023 LC map. Based on the comparison, the changes that occurred in 35 years are presented quantitatively.

4.1 Kuching LC Pattern in 1988

The LC map layout generated from the Landsat TM image is displayed in Figure 4a. The classification categories for 1988 and their area information are listed in Table 3. Based on the results, the largest category was agriculture land (201,225.76 ha, 45.43% of the total area), followed by forest land (178,369.48 ha, 43.41% of the total area), barren land (15,240.31 ha, 3.71% of the total area), water bodies (9,842.57 ha, 2.40% of the total area) and urban land (6,200.71 ha, 1.51% of the total area).

Table 3. Confusion Matrix for the produced 1988 LC Map of the study area.

	Reference Data							
Classified Data	Cloud	Water Bodies	Forest Land	Barren Land	Urban Land	Agriculture Land	Row Total	User Accuracy (%)
Cloud	10.00	0.00	0.00	0.00	0.00	0.00	10.00	100.00
Water Bodies	0.00	9.00	1.00	0.00	0.00	0.00	10.00	90.00
Forest Land	0.00	0.00	91.00	0.00	0.00	8.00	99.00	91.92
Barren Land	0.00	0.00	0.00	9.00	0.00	0.00	9.00	100.00
Urban Land	0.00	0.00	0.00	1.00	8.00	0.00	9.00	88.89
Agriculture Land	0.00	0.00	11.00	0.00	0.00	112.00	123.00	91.06
Column Total	10.00	9.00	103.00	10.00	8.00	120.00	260.00	
Producer Accuracy (%)	100.00	100.00	88.35	90.00	100.00	93.33		
Overall Accuracy (%)					**91.92**			
Kappa Statistics					**0.8709**			

4.2 Kuching LC Pattern in 2023

The classified image for 2023 (Figure 4b) was produced using the Landsat 9 image. According to the results, the Kuching division area mainly consisted of agricultural land (186,642.53 ha, 48.97% of the total area), followed by forest land (181,446.65 ha, 44.16% of the total area). Urban land rose to the third place, with 5.39% of the total area, covering 22,144.76 ha. Water bodies are 10,692.94 ha, 2.60% of the total area. Finally, barren land areas are 9,951.95 ha, which makes

2.42% of the total area. The classification categories for 2023 and their area information are listed in Table 4. From 1988 to 2023, the LC patterns changed significantly.

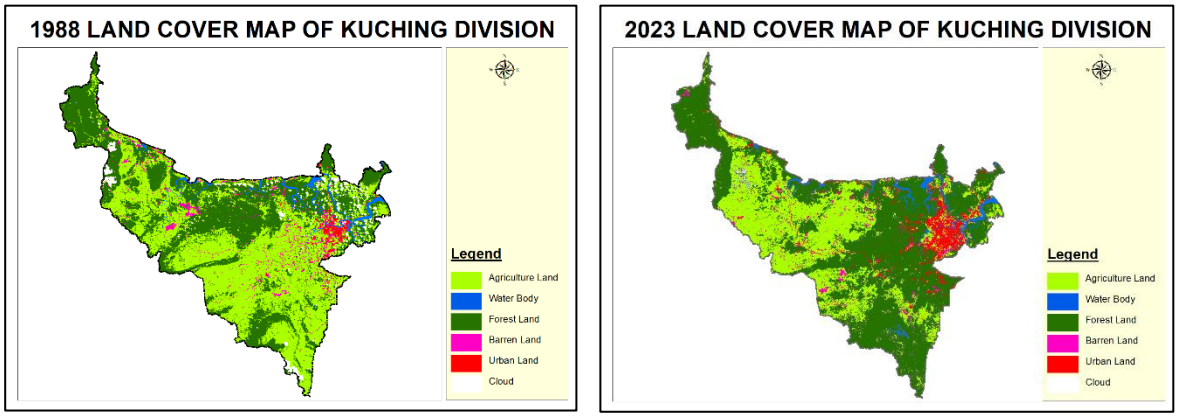

(a) LC map of the study area in 1988. (b) LC map of the study area in 2023.

Figure 4. Classification output using Support Vector Machine algorithm.

Table 4. Confusion Matrix for the produced 2023 LC Map of the study area.

	Reference Data							
Classified Data	Cloud	Water Bodies	Forest Land	Barren Land	Urban Land	Agriculture Land	Row Total	User Accuracy (%)
Water Bodies	10.00	0.00	0.00	0.00	0.00	0.00	10.00	100.00
Cloud	0.00	10.00	0.00	0.00	0.00	0.00	10.00	100.00
Forest Land	0.00	0.00	104.00	0.00	1.00	5.00	110.00	94.55
Barren Land	0.00	0.00	0.00	9.00	1.00	0.00	10.00	90.00
Urban Land	1.00	0.00	0.00	1.00	12.00	0.00	14.00	85.71
Agriculture Land	1.00	0.00	6.00	0.00	0.00	92.00	99.00	92.93
Column Total	12.00	10.00	110.00	10.00	14.00	97.00	253.00	
Producer Accuracy (%)	83.33	100.00	94.55	90.00	85.71	94.85		
Overall Accuracy (%)					**93.68**			
Kappa Statistics					**0.9031**			

4.3 Kappa Coefficient and Overall Accuracy for 1988 and 2023 Imageries

An accuracy assessment was performed on both 1988 and 2023 LC maps. For the 1988 LC map, 260 pixels were selected randomly using the stratified random sampling method. It had a kappa

statistic of 0.8709 and an overall accuracy of 91.92% (Table 3). The producer's accuracy for each class was higher than 80%. The user's accuracy for all classes was higher than 85%.

For the 2023 LC map, 253 pixels were randomly selected. The kappa statistics and overall accuracy of the 2023 LC map were 0.9031 and 93.68%, respectively (Table 4). The producer's accuracy for each class was higher than 80%, and the user's accuracy for every class was higher than 85%. The accuracy for each class was observed to be satisfactory in both classifications. Both classification maps produced higher than 80% Kappa values, indicating good classification performance (Lillesand *et al.*, 2004; Jensen, 2005). Kappa values also tell us how well the classification process performed compared to a random assignment of values (Tammy *et al.*, 2023).

4.4 Change Detection from 1988 to 2023

The area for each LC class and its changes from 1988 to 2023 are presented in Table 5. Figure 5 displays the spatial expansion of the urban land. In 2023, the area for urban land has increased massively compared to 1988. Positive and negative changes were observed over 35 years in the study area. The agricultural land and barren land categories decreased in their area, whereas the urban land, forest land, and water bodies categories increased.

As displayed in Table 5, the most substantial changes in area were observed for the urban land category, followed by agriculture land, barren land, forest land, and water bodies categories. Figure 10 shows the graph depicting the land cover changes in percentage of the study area.

4.4.1 Urban Land

The urban land increased significantly from 6,200.71 ha in 1988 to 22,144.76 ha in 2023, representing a net increase of 15,944.05 ha. This urban land increased due to the rise in population, demand for shelter by inhabitants, and tourism activities. Another reason for growth is that the study area is in Kuching, the capital city of Sarawak, where the demand for development is higher than that of other places in Sarawak.

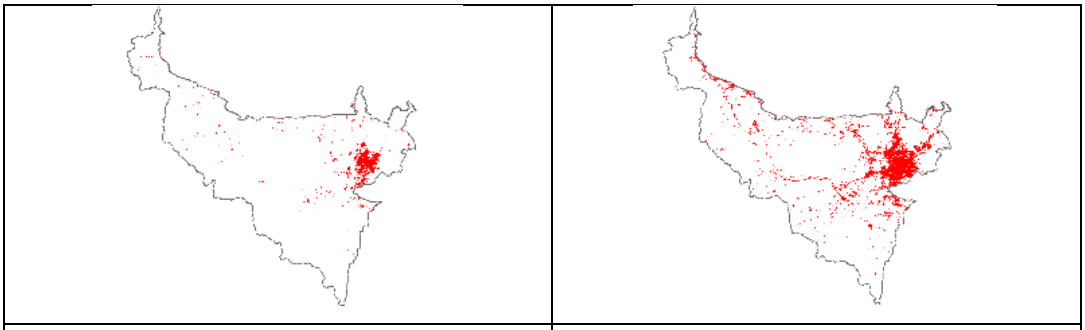

Figure 5. Expansion of urban land from 1988 to 2023.

4.4.2 Water Bodies

The area for water bodies increased from 9,842.57 ha in 1988 to 10,692.94 ha in 2023, representing a net increase of 850.37 ha (Figure 6). The increase is due to the conversion from other land categories into water bodies over the past 35 years.

One of the main factors is the completion of Bengoh Dam's impoundment in 2015. Flooded areas from the dam have increased the number of water bodies in the affected area. The development of aquaculture ponds built in mangrove areas is another reason for the increase in the water bodies areas. This development activity aligns with the policy of developing commercial aquaculture by establishing the Sarawak Aquaculture Industrial Zone (AIZ).

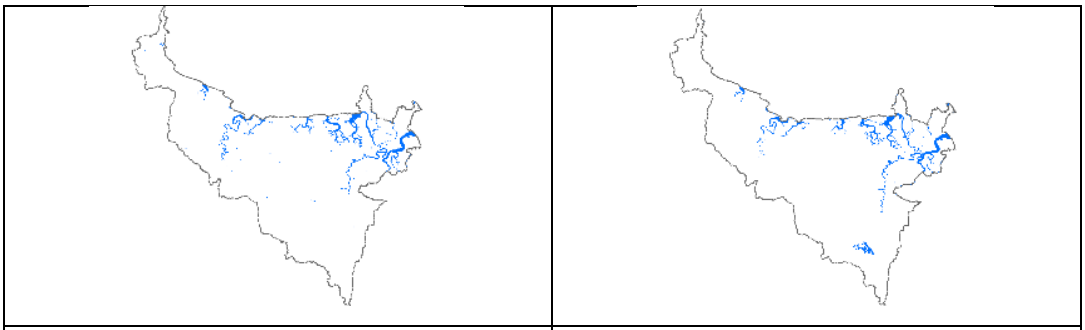

Figure 6. Expansion of water bodies area from 1988 to 2023.

4.4.3 Agriculture Land

The land area of agriculture decreased (Figure 7) from 201,225.76 ha in 1988 to 186,642.53 ha in 2023, representing a net decrease of 14,583.22 ha. The available agricultural land is due to the demand for urban development and changes in cultivation to forest land. Some of the former land

used for cultivation, such as paddy, rubber, pepper, etc., in rural areas has been abandoned and become forest land because people migrate to cities/ urban areas.

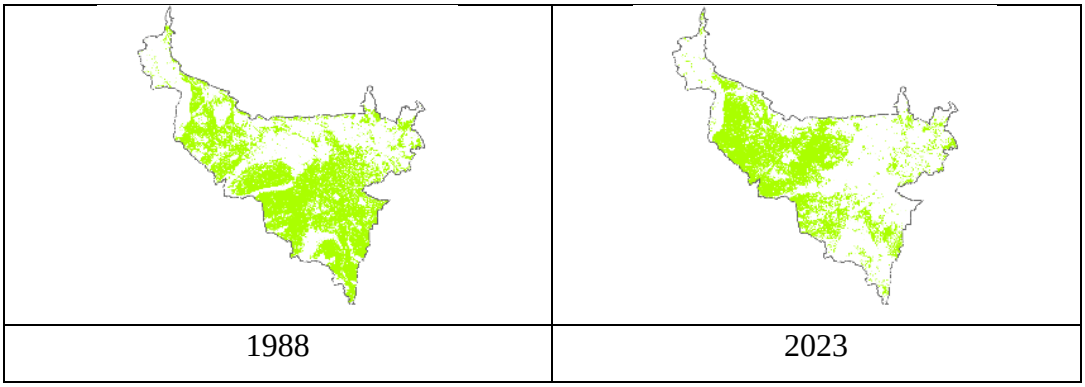

Figure 7. Degradation of agricultural land from 1988 to 2023.

4.4.4 Forest Land

Forest land areas increased from 178,369.48 ha in 1988 to 181,446.65 ha in 2023, representing a net increase of 3,077.17 ha (Figure 8). This incremental increase is attributed to converting agricultural land to forest land. Some of the land is no longer cultivated and has become forest land. The reforestation of former logging areas also contributed to increased forest land in the study area.

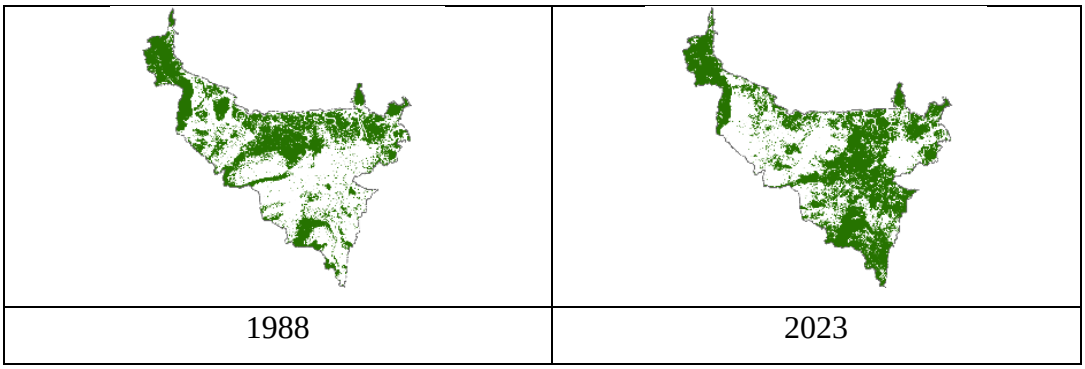

Figure 8. Expansion of forest land from 1988 to 2023.

4.4.5 Barren Land

Barren land areas decreased from 15,240.31 ha in 1988 to 9,951.95 ha in 2023, representing a net decrease of 5,288.37 ha (Figure 9). The degradation of barren land is attributed to the conversion into urban and agricultural land. The cleared land has become urban land, such as town buildings,

shophouses, etc. Some barren land removed for plantation has also been grown, such as oil palm, paddy, and other agricultural land.

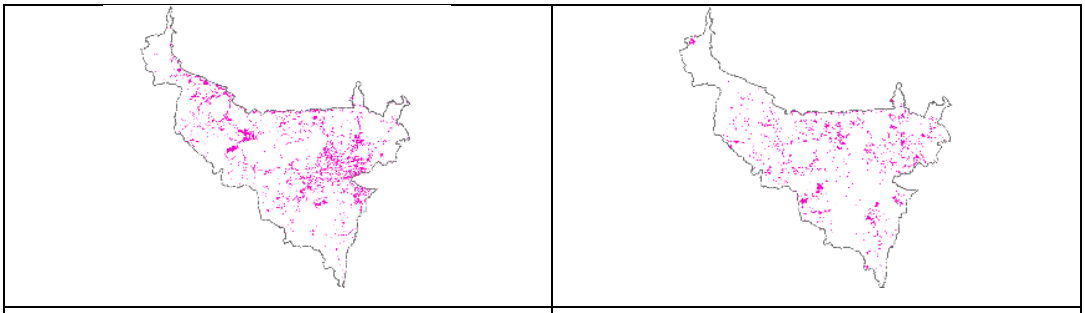

1988	2023

Figure 9: Degradation of barren land from 1988 to 2023.

Table 5. The area for each LC class in the 1988 and 2023 data sets has changed over 35 years.

No	Class Name	LC Area (ha)		Area Changed (ha) (2023-1988)	Percent change (%)
		1988	2023		
1	Agriculture Land	201,225.76	186,642.53	-14,583.22	-3.55
2	Barren Land	15,240.31	9,951.95	-5,288.37	-1.29
3	Forest Land	178,369.48	181,446.65	+3,077.17	0.75
4	Urban Land	6,200.71	22,144.76	+15,944.05	3.88
5	Water Body	9,842.57	10,692.94	+850.37	0.21

(+) Indicates an increase, and (−) indicates a decrease in the area under an LC class over 35 years (1988–2023)

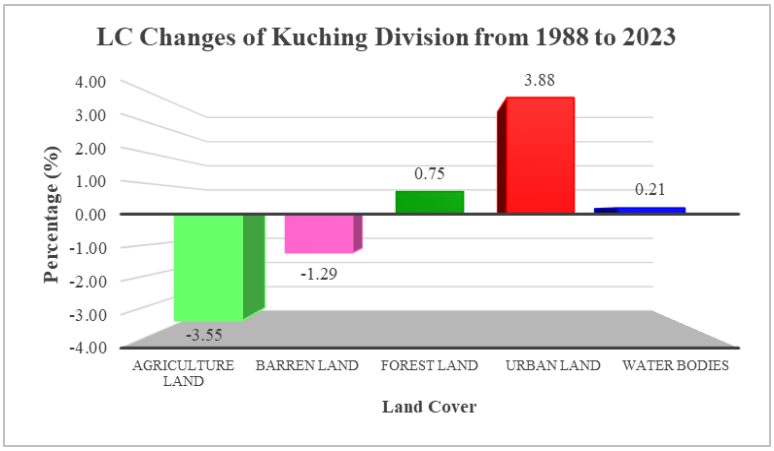

Figure 10: Graph showing the land cover changes percentage of the study area.

5.0 Conclusion and Future Work

Classification of satellite images to identify and map land cover changes in Kuching Division over 35 years from 1988 to 2023 was successfully carried out in the present study. Land cover changes accuracy assessment was performed using a confusion matrix, with a significant accuracy of over 85% for each class. This study found that the main class of land use change in Kuching is urban land, with an increase of 3.88%, as Kuching is the capital city of Sarawak. The study successfully presents LC changes and future predictions highlighting significant patterns of land use change in the Kuching Division. This information could be helpful for land use/land cover administration and future planning under the Sarawak State Post COVID-19 Development Strategy (PCDS) 2030. To enhance this study further, several approaches can be considered: developing a land cover classification method using deep learning, utilizing high-resolution satellite imagery to increase detail and accuracy in distinguishing land cover types, and generating a trend analysis of land cover classification over the selected time range. Regarding environmental concerns, it is recommended that the scope of the study be expanded to explore the relationship between urban growth and land surface temperature (LST). This would provide insights into how urbanization affects the local thermal environment and help develop strategies to manage and mitigate the effects of urban heat islands.

Acknowledgements

The authors sincerely thank the Department of Land and Survey, Sarawak (LSD) for providing the 1992 S22 Land Use map of Kuching, Sarawak. We would also like to acknowledge the LIMPAS team from MYSA and LSD for producing the SS30 Land Cover map of Sarawak, which we used as one of the references for this study. Landsat TM and OLI data products were downloaded for free from the EarthExplorer website.

Reference

Abbas Taati, Fereydoon Sarmadian, Amin Mousavi, Chamran Taghati Hossien Pour, and Amir Hossein Esmaile Shahiee. (2015). Land Use Classification using Support Vector Machine and Maximum Likelihood Algorithms by Landsat 5 TM Images. Walailak Journal of Science and Technology (WJST) 12(8). 681-687. DOI:10.14456/WJST.2015.33.

Rokni Deilmai, B., Ahmad, B.B and Zabihi,H. (2014) Comparison of two Classification methods (MLC and SVM) to extract land use and land cover in Johor Malaysia. IOP Conference Series: Earth and Environmental Science, Volume 20, 7th IGRSM International Remote Sensing & GIS Conference and Exhibition 22–23 April 2014, Kuala Lumpur, Malaysia.

Bolin Fu, Hang Yao, Feiwu Lan, Sunzhe Li, Yiyin Liang, Hongchang He, Mingming Jia, Yeqiao Wang & Donglin Fan (2023) Collaborative multiple change detection methods for monitoring the spatio-temporal dynamics of mangroves in Beibu Gulf, China, GIScience & Remote Sensing, 60:1, 2202506, DOI: 10.1080/15481603.2023.2202506

Congalton, R.G. and K. Green. (1999). Assessing the Accuracy of Remotely Sensed Data: Principles and Practices. Lewis Publishers. 137 pp.

Dires Tewabe & Temesgen Fentahun | (2020) Assessing land use and land cover change detection using remote sensing in the Lake Tana Basin, Northwest Ethiopia, Cogent Environmental Science, 6:1, 1778998, DOI: 10.1080/23311843.2020.1778998

Economic Planning Unit Sarawak. (2021). Post COVID-19 Development Strategy 2030. https://sarawak.gov.my/media/attachments/PCDS_Compressed_22_July_2021.pdf

ESRI. (2021). Image Classification using the ArcGIS Spatial Analyst Extension. https://desktop.arcgis.com/en/arcmap/latest/extensions/spatial-analyst/image-classification/image-classification-using-spatial-analyst.htm

Vivekananda, GN, Swathi, R. & Sujith, AVLN (2021) Multi-temporal image analysis for LULC classification and change detection, European Journal of Remote Sensing, 54:sup2, 189-199, DOI: 10.1080/22797254.2020.1771215.

Jean-François Mas, Richard Lemoine-Rodríguez, Rafael González-López, Jairo López-Sánchez, Andrés Piña-Garduño & Evelyn Herrera-Flores (2017) Land use/land cover change detection combining automatic processing and visual interpretation, European Journal of Remote Sensing, 50:1, 626-635, DOI: 10.1080/22797254.2017.1387505

Jenness, J., and J.J. Wynne. 2005. Cohen's Kappa and classification table metrics 2.0: an ArcView 3x extension for accuracy assessment of spatially explicit models: U.S. Geological Survey Open-File Report OF 2005-1363. U.S. Geological Survey, Southwest Biological Science Center, Flagstaff, AZ.

Jensen, J. R. (2005). "Introductory Digital Image Processing: A Remote Sensing Perspective". Prentice Hall, NJ: Pearson.

Jun Chen, Jin Chen, Anping Liao, Xin Cao, Lijun Chen, Xuehong Chen, Chaoying He, Gang Han, Shu Peng, Miao Lu, Weiwei Zhang, Xiaohua Tong, Jon Mills. (2014). Global land cover mapping at 30 m resolution: A POK-based operational approach. ISPRS Journal of Remote Sensing 103 (2015) 7-27. http://dx.doi.org/10.1016/j.isprsjprs.2014.09.002.

Kemarau R. A. and Eboy O. V. (2021). Land Cover Change Detection in Kuching, Malaysia using Satellite Imagery. Borneo Journal of Sciences and Technology Volume (3), Issue (1), Pages 61-65.

Knudby A.J. (2021). Remote Sensing. https://ecampusontario.pressbooks.pub/remotesensing/chapter/chapter-7-accuracy-assessment/

Land Survey Department Sarawak & Malaysian Space Agency. (2023). LIMPAS: Pendigitalan Dimensi Bumi Dari Angkasa. ISBN 978-967-16181-4-1.

Lillesand, T.M., Kiefer, R.W. and Chipman, J.W., (2004). "Remote Sensing and Image Interpretation". 5th Edition, John Wiley & Sons Inc., New York.

Ling, J.; Zhang, H.; Lin, Y. Improving Urban Land Cover Classification in Cloud-Prone Areas with Polarimetric SAR Images. Remote Sens. 2021, 13, 4708. https:// doi.org/10.3390/rs13224708

Seyam, M.M.H., Haque,M.R. and Rahman, M.M. (2023). "Identifying the land use land cover (LULC) changes using remote sensing and GIS approach: A case study at Bhaluka in Mymensingh, Bangladesh," Case Studies in Chemical and Environmental Engineering, p. 100293, doi: https://doi.org/10.1016/j.cscee.2022.100293.

Seyam, M.M.H, Rashedul Haque, Md and Md Mostafizur Rahman, Md. (2023). Identifying the land use land cover (LULC) changes using remote sensing and GIS approach: A case study at Bhaluka in Mymensingh, Bangladesh. Case Studies in Chemical and Environmental Engineering. Volume 7. https://doi.org/10.1016/j.cscee.2022.100293.

Nurul Suliana Ahmad Hazmi, Shahruddin Ahmad, Maizatuldura Mohd Isa, Hana Mohamed Jamil, Roslinah Samad and Shimatun Jumani Ibrahim. (2021). Assessment Of Land Surface Temperature in Dry and Wet Season Using Sentinel Imageries in Cameron Highlands, Malaysia. 42nd Asian Conference on Remote Sensing 22-26 November 2021. Can Tho, Vietnam.

Osuna and R Freud (1977). Support Vector Machines: Training and Applications. Massachusetts Institute of Technology Cambridge, USA, p. 1-144.

Roy, P.S and Roy, A. (2010). Land use and land cover change in India: A remote sensing & GIS Perspective. Journal of the Indian Institute of Science VOL 90:4 Oct-Dec 2010.

Parece T & McGee J. (2023). Remote Sensing With ArcGIS Pro (Second Edition). https://pressbooks.lib.vt.edu/remotesensing/chapter/chapter-25-accuracy-assessment/

Radhakrishnan, N., Satish Kumar, E., & Kumar, S. (2014). Analysis of urban sprawl pattern in Tiruchirappalli city using applications of remote sensing and GIS. Arabian Journal Science and Engineering, 39(7), 5555–5563. https://doi.org/10.1007/s13369-014-1099-2

Steven E. Franklin, Oumer S. Ahmed, Michael A. Wulder, Joanne C. White, Txomin Hermosilla & Nicholas C. Coops (2015) Large Area Mapping of Annual Land Cover Dynamics Using Multitemporal Change Detection and Classification of Landsat Time Series Data, Canadian Journal of Remote Sensing, 41:4, 293-314, DOI: 10.1080/07038992.2015.1089401

The Official Portal of Sarawak Government. (2020). Sarawak Population (https://sarawak.gov.my/web/home/article_view/240/175/)

USGS. (2013, March). Landsat Missions – Landsat 8. https://www.usgs.gov/core-science-systems/nli/landsat/landsat-8.

USGS. (n.d). Landsat Missions - Landsat 5. https://www.usgs.gov/landsat-missions/landsat-5

USGS. (n.d.). EarthExplorer. https://earthexplorer.usgs.gov/

W.M.D.C.Wijesinghe and W.K.N.C. Withanage. (2021). Detection of the changes of land use and land cover using remote sensing and GIS in Thalawa DS Division. Prathimana Journal Volume 14, No.1, 2021, 072 – 086.

Yang, Y.; Yang, D.; Wang, X.; Zhang, Z.; Nawaz, Z. Testing Accuracy of Land Cover Classification Algorithms in the Qilian Mountains Based on GEE Cloud Platform. Remote Sens. 2021, 13, 5064. https://doi.org/10.3390/ rs13245064

.